The Crystal Structure of Catechol Oxidase: New Insight into the Function of Type-3 Copper Proteins

CARSTEN GERDEMANN,[†,‡] CHRISTOPH EICKEN,[†,‡,§] AND BERNT KREBS*[,†]

Institut für Anorganische und Analytische Chemie der Universität Münster, Wilhelm-Klemm-Strasse 8, 48149 Münster, Germany, and Institut für Biochemie der Universität Münster, Wilhelm-Klemm-Strasse 2, 48149 Münster, Germany

Received March 9, 2001

ABSTRACT

The crystal structure of catechol oxidase reveals new insight into the functional properties of the type-3 copper proteins. This class of proteins includes the closely related and better-known tyrosinase as well as hemocyanin, an oxygen transport protein. All these proteins have a dinuclear copper center, have similar spectroscopic behaviors, and show close evolutionary and functional relationships. Comparison between the 3D structures of catechol oxidase and hemocyanins reveals the structural reasons for the divergence in function.

1. Introduction

Dioxygen and Metalloproteins. Transport, activation, and metabolism of dioxygen are very important processes in most living organisms. These functions are often realized by metalloproteins containing iron or copper. Iron-containing heme proteins include the best-known examples of this type, e.g., hemoglobin and myoglobin (dioxygen transport), cytochrome *c* oxidase (activation and reduction of dioxygen), and peroxidase (elimination of radical intermediates). Other metalloproteins with an iron- or copper-containing dinuclear metal center serve as biological alternatives. Examples of this type of protein are the two dioxygen transport proteins, hemerythrin (iron) and hemocyanin (copper). The dinuclear metal centers in these proteins are closely similar to the active sites of other proteins, whose function is not dioxygen transport but enzymatic catalysis.

The Three Classical Types of Copper Centers in Proteins. Based on their spectroscopic characteristics, three types of active site are distinguished in copper proteins.[1] The type-1 copper centers—so-called "blue copper centers"—are found in electron-transfer proteins such as plastocyanin and azurin. Their deep blue color is caused by an intense Cys S−Cu(II) charge-transfer transition ($\epsilon > 2000\ cm^{-1}\ M^{-1}$). In the EPR spectrum, the parallel $^{63}Cu^{65}Cu$ hyperfine splitting is much smaller than the value for hexaaqua Cu(II) complexes. Crystal structures of blue copper proteins indicate that the metal centers have a strongly distorted tetrahedral coordination sphere with differences of up to 22° from the ideal tetrahedron angle.[2] This is interpreted as corresponding to a "transition state" between the favored coordination geometries of Cu(II) (square-planar) and Cu(I) (tetrahedral).

The "non-blue copper centers" form the class of type-2 centers. They are found in oxidases such as galactose oxidase and in oxygenases such as dopamine-β-monooxygenase. In addition, a type-2 copper center appears in the dinuclear metal site of Cu,Zn-superoxide dismutase. Type-2 copper centers are characterized by a square-planar coordination sphere. They show the spectroscopic behavior of copper(II) known from the Cu(II) hexaaqua complex (UV/vis, EPR). In contrast to these mononuclear copper sites, the type-3 copper centers contain two copper atoms and are described in detail in the next section.

Some copper proteins—e.g., laccase, ascorbate oxidase, and ceruloplasmin—do not belong to these three classical types.[3] The copper sites in these proteins include a trinuclear copper moiety often described as a combination of a type-2 and a type-3 center. In ascorbate oxidase, a type-1 copper center is about 13 Å distant from such a trinuclear copper unit.[4] Yet two other types of copper sites—CuA and CuB—are found in cytochrome *c* oxidase, which also has several non-copper metal centers.[3]

In Detail: Proteins with a Type-3 Copper Center. Proteins with type-3 copper centers can serve either as oxygenase/oxidase enzymes or as dioxygen transport proteins.[5] An example of an oxygen carrier protein is hemocyanin (HC), a well-known member of this class of copper proteins. HCs can be divided into two classes depending on their biological source: the arthropodan (e.g., lobsters and spiders) and the molluscan (e.g., octopus and snails) hemocyanins. These have different subunit organizations and only a weak evolutionary

Carsten Gerdemann was born in Münster, Germany, in 1970. He received his diploma in chemistry from the University of Münster in 1997. He recently received his Ph.D. in chemistry at the University of Münster, studying sequencing and modeling of catechol oxidase.

Christoph Eicken was born 1967 in Aachen, Germany. He studied chemistry at the University of Münster and received his Ph.D. in 1999. During his Ph.D. work in Bernt Krebs's group, he solved the 3D structure of catechol oxidase. Afterward he joined James C. Sacchettini's group at Texas A&M as a post-doc, first in College Station and now in Houston at The Center for Structural Biology. His current main focus is on proteins involved in Lyme disease and tuberculosis.

Bernt Krebs was born 1938 in Gotha, Germany. He received his Ph.D. in chemistry from the University of Göttingen in 1965. After postdoctoral research with W. A. Hamilton at Brookhaven National Laboratory, he got his Habilitation at the University of Göttingen in 1969. He became Professor of Inorganic Chemistry at the University of Kiel in 1971. He moved to the University of Bielefeld in 1973 and to the University of Münster in 1977, where he is Professor of Inorganic Chemistry and Director of the Institute of Inorganic Chemistry. His research is primarily focused on bioinorganic coordination chemistry, on X-ray structure analysis of model compounds and its related metalloenzymes.

* To whom correspondence should be addressed. Phone: +49 (251) 8333131. Fax: +49 (251) 8338366. E-mail: krebs@uni-muenster.de.

† Institut für Anorganische und Analytische Chemie der Universität Münster.

‡ Institut für Biochemie der Universität Münster.

§ Present address: The Center for Structural Biology, Albert B. Alkek Institute of Biosciences and Technology, Texas A&M University, 2121 W. Holcombe Blvd., Houston, TX 77030-3303.

10.1021/ar990019a CCC: $22.00
Published on Web 02/07/2002

Scheme 1. Reaction Pathway of the Oxygenation and Oxidation Catalyzed by TYR and CO

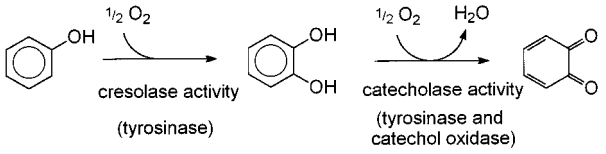

relationship.[6] For several years, the HCs from two arthropods, spiny lobster[7] and horseshoe crab,[8] were the only HCs for which crystal structures were available. Recently, a subunit from a molluscan HC (giant octopus) could be crystallized and its 3D structure determined.[9]

Catechol oxidase (CO), also known as *o*-diphenol oxidase, is a less well known member of the type-3 copper proteins.[5] The official nomenclature is 1,2-benzenediol: oxygen oxidoreductase, indicating that dioxygen is the second substrate. CO catalyzes exclusively the oxidation of catechols (i.e., *o*-diphenols) to the corresponding *o*-quinones (called catecholase activity, Scheme 1). In contrast to CO, the strongly related tyrosinase (TYR)—another member of the type-3 copper proteins—shows additional monooxygenase activity (Scheme 1). This so-called cresolase activity enables the enzyme to accept also monophenols (like tyrosine or cresol) as substrates. COs are found in plant tissues and in some insects and crustaceans,[10] whereas TYRs can be isolated from a broader variety of plants, fungi, bacteria, mammalians, crustaceans, and insects.[5,10] The differentiation between CO and TYR is not rigorous, as some plant COs also show weak monooxygenase activity. However, these COs often do not accept tyrosine as a substrate.[11,12] Nevertheless, COs are sometimes described as TYRs and, in addition, the names polyphenol oxidase (PPO), diphenol oxidase, and phenol oxidase are used for both enzymes. These designations are avoided here as they lack the necessary precision in differentiating between TYR/CO and laccase. Laccase is also called PPO as it catalyses the oxidation of *p*-diphenols.[11−13] The Nomenclature Committee of the International Union of Biochemistry and Molecular Biology distinguishes between cresolase activity (E.C. 1.14.18.1) and catecholase activity (1.10.3.1), but not between TYR and CO.[11]

The functional and structural differences between TYR, CO, and HC could not be rationalized for a long time, as detailed structural information was available only for arthropodan HCs. The 3D structure of TYR is not yet known, but the recent structural data for a molluscan HC and a plant CO allow a deeper insight into the active site of type-3 copper proteins.

2. Molecular Properties of Plant COs

Purification and Molecular Weight. The first CO was isolated in 1937.[11] Subsequently, COs were purified from a broad spectrum of plants and fruits (e.g., potato, spinach, apple, grape berry[11]), and more recently also from gypsy wort[14] and litchi fruit.[15] The purity of the COs was not always satisfactory due to a multiplicity of isozymes and forms,[11] but improved purification protocols have been reported, e.g., for CO from black poplar.[14]

For CO from sweet potatoes *Ipomoea batatas* (ibCO), several isozymes were found in 1965.[16] Later, a CO with 33 kDa molecular mass was purified from sweet potato. It was first proposed to be a *p*-coumaryl-D-glucose hydroxylase, but it was later renamed CO (or PPO in the original citations).[17] The isolation and purification to homogeneity of two further isozymes (separate gene products with molecular mass 39 and 40 kDa, respectively) were reported recently.[18] The detailed characterization of these two isoforms of ibCO included a determination of the crystal structure of the 39 kDa isoform.[19]

The molecular weight of CO varies, depending on the tissue and organism. Two ranges of molecular mass can sometimes be found, even in a single source: one in the range of 38−45 kDa, and a second in the range of 55−60 kDa. This is possibly due to C-terminal processing (see below). Smaller enzymes with a molecular weight of about 30 kDa are also found, but they are generally described as proteolyzed derivatives of the purified mature protein.

Primary Structure and DNA Sequence of CO, TYR, and HC. The cDNA of plant COs consists of three translated regions encoding the transit peptide of about 9 kDa leading into the chloroplasts, the mature protein, and an additional C-terminal extension peptide of unknown function. This C-terminal extension peptide of about 15 kDa is cleaved off by the plant or during purification.[11] However, no protein responsible for cleavage of the peptide could be identified, and the function and control of the cleavage remain unclear. A similar C-terminal extension was found in TYRs from bacteria, and it was postulated that cleavage of this extension peptide activates the enzyme.[20]

On the basis of the biological source of the proteins, seven different domain organizations could be identified (Figure 1). TYRs and COs from higher eukaryotes and plants have all three domains and differ only in some characteristic regions encoding the C-terminal extension peptide. TYRs from fungi and bacteria lack a transit peptide encoding domain.[20] In addition, TYRs from bacteria have a shorter sequence, leading to a mature protein with a mass <30 kDa. TYRs and COs from insects and crustaceans are different from the four mentioned previously but are related to arthropodan HCs. They also show a latent form, but in contrast to plant COs they are activated by cleavage of a N-terminal region. Both classes of HCs show additional regions compared to the correlated TYRs and COs.

Plant COs of different organisms have a sequence identity of about 40−60%. The sequence identity between plant COs and molluscan HCs is also worth mentioning (about 35% over almost the entire length of the sequences). In contrast, the sequence identity between plant COs and other type-3 copper proteins from any nonplant source is limited to the two copper-binding regions.

The two copper-binding regions show the highest conservation throughout all type-3 copper proteins. Es-

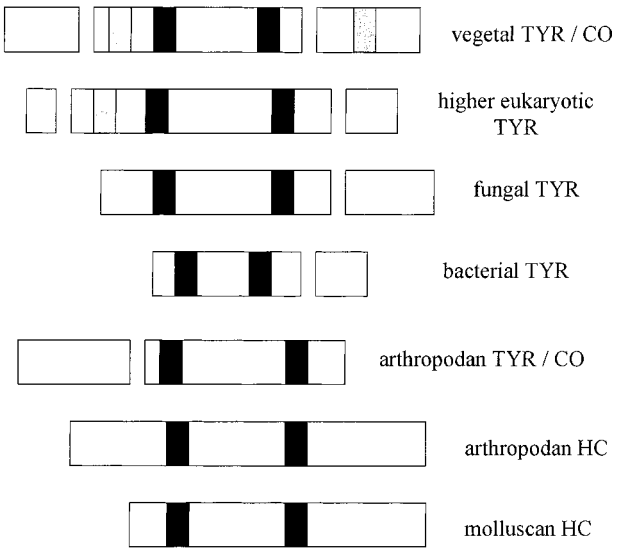

FIGURE 1. Primary structure of type-3 copper proteins. Lengths of the segments are proportional to the numbers of amino acid residues. Copper-binding histidine-rich regions are shown in black, cysteine-rich in light gray, and the additional histidine-rich region on the C-terminal extension peptide of plant CO in dark gray.

pecially the region binding CuB is highly conserved, whereas the CuA binding region shows more sequence variety and has been held responsible for the differing functions of TYR, CO, and HC.[20] Both copper-coordinating regions are shown in Figure 2.

Additional Activities of Type-3 Copper Proteins. As outlined before, the three kinds of type-3 copper enzyme are strongly related to one another. This is also indicated by the fact that some HCs have weak catecholase activity or can be proteolytically activated to induce such activity.[6,21] Weak catecholase activity has often been found for molluscan HCs, e.g., *Octopus vulgaris* HC,[22] for some arthropodan HCs,[21] and for HC from tarantula after partial proteolytic digestion with trypsin or chymotrypsin.[21] In the case of tarantula HC, the authors suggest that the activation is the result of proteolytic cleavage of a N-terminal region.

Further, as stated above, some plant COs show weak cresolase activity detectable by use of special monophenols such as 4-hydroxyanisole.[23] This activity often seems to be reduced or lost during purification, possibly as a result of structural changes at the active site.[11] Finally, weak additional catalase activity, i.e., the dismutation of hydrogen peroxide, has been detected for HC, TYR, and CO.[24]

3. The Dimetal Site

Spectroscopic Characterization. In the *met* state (Cu(II)−Cu(II)) of CO and TYR, the two copper atoms are antiferromagnetically coupled ($-2J > 600$ cm^{-1}) with an $S = 0$ EPR ground state, which is characteristic for copper of type-3. An EPR signal typical for Cu(II) is detectable only after denaturation of the protein.[18] The blue-colored *oxy* state formed after binding of dioxygen or hydrogen peroxide is characterized by absorption maxima at 343 nm ($\epsilon \approx 6500$ cm^{-1} M^{-1}), assigned to an O_2^{2-} ($\pi_\sigma^\times$) → Cu(II) charge-transfer transition, and at 580 nm ($\epsilon \approx 450$ cm^{-1} M^{-1}), corresponding to an O_2^{2-} ($\pi_\nu^\times$) → Cu(II) charge-transfer transition. (Both extinction coefficients are cited for the copper atoms of ibCO.[18]) The reduced Cu(I)−Cu(I) state (*deoxy* state) shows no antiferromagnetically coupled copper atoms and no bridging atom.

The resonance Raman spectrum of *oxy*CO from black poplar leaves (*Populus nigra*) has its strongest peak at 277 cm^{-1}. This observation agrees with the UV resonance Raman spectra of *oxy*TYR and *oxy*HC, where a corresponding peak was assigned to the Cu−N_{ax} (axial His) stretching mode.[14]

EXAFS measurements on ibCO have revealed a Cu−Cu distance of 2.9 Å for the *met* form and are consistent with a coordination sphere containing three histidines and one oxygen for each copper. For the *oxy* state of ibCO, EXAFS measurements indicate a Cu−Cu distance of 3.8 Å and coordination by five N/O atoms.[18] EXAFS and XANES spectra for the *oxy* form of *Neurospora crassa* TYR lead to a Cu−Cu distance of 3.6 Å.[5]

Recently, ^{1}H NMR spectra have been measured for *Streptomyces antibioticus* TYR, revealing the coordination of each copper atom by the N_ϵ atoms of three histidine residues.[25] Binding of chloride to TYR was also detected, but the nature of this binding is not yet clear.

Model Compounds Simulating the Properties of Type-3 Copper Centers. Model compounds were important for the elucidation of the binding mode of dioxygen to the copper center in the *oxy* state. It was proposed that dioxygen is bound in the peroxide oxidation state, either as cis-μ-η^1:η^1 (O_2^{2-} bridging as the molecule) or as μ-η^2:η^2 (O_2^{2-} localized between the two Cu atoms, Figure 3). The former mode was found in a model compound,[26] and the latter was modeled using [Cu(HB(3,5-i-Pr$_2$pz)$_3$]$_2$(O_2) (Figure 3a).[27] The diamagnetism and spectroscopic behavior of this second model compound resembled those of *oxy*HC. Finally, an X-ray structural analysis of *oxy*HC from horseshoe crab (*Limulus polyphemus*, see below) proved the μ-η^2:η^2 binding mode to be correct (Figure 3b).[8]

Recent developments in model chemistry afforded the crystal structure of a model compound that is stable at room temperature and binds dioxygen reversibly, thus reproducing the capability of HC.[28] Complexes to be considered as functional models for TYR could also be crystallized. First, a model compound capable of hydroxylating an aromatic ring of the ligand was reported.[26,28] Other model compounds showing cresolase and catecholase activity on mono- and diphenols, respectively, were crystallized.[29] In contrast, catecholase activity on 3,5-di-*tert*-butylcatechol without cresolase activity could be simulated using several model compounds. A bidentate binding mode was found for tetrachloro-*o*-catechol in a crystal structure and was suggested as a model for intermediates in the mechanism of catechol oxidation. However, all model compounds synthesized so far only achieve turnover numbers about 10 000-fold lower than the native enzymes.[26]

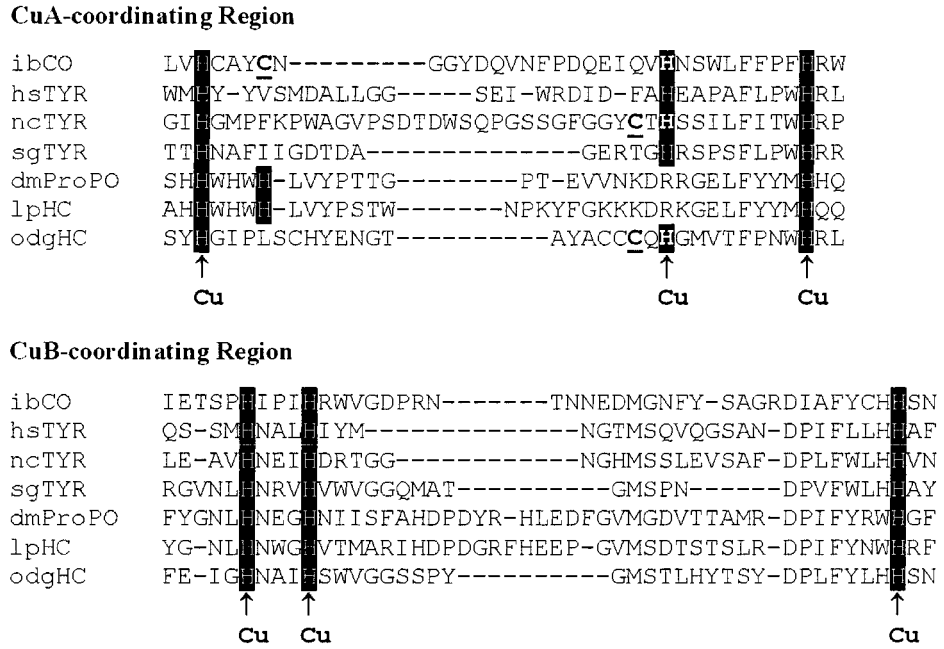

FIGURE 2. Sequence alignment of the copper-coordinating regions of the type-3 copper proteins shown in Figure 1. Residues forming thioether bonds[35] are marked in bold letters, copper-coordinating histidine residues inverse. Abbreviations: ibCO, CO from sweet potato (*Ipomoea batatas*); hsTYR, human (*Homo sapiens*) TYR; ncTYR, TYR from *Neurospora crassa*; sgTYR, TYR from *Streptomyces glaucescens*; dmProPO, Pro-phenoloxidase from fruit fly (*Drosophila melanogaster*); lpHC, HC from horseshoe crab (*Limulus polyphemus*); odgHC, HC from giant octopus (*Octopus dofleini*), subunit *g*.

Kinetic and Inhibition Studies on Plant CO. There are some detailed kinetic and substrate specifity studies on CO and TYR, but the main kinetic interest was focused on TYR.[30] Plant protein representatives were also investigated in terms of reaction kinetics and activation. Detailed studies on substrate specificity were performed for isozymes from potato, tea, pears,[11] dates,[12] and gypsy wort.[31] ibCO shows high activity, especially for catechol, 4-methylcatechol, and caffeic acid.[18] Activation of the latent form is induced by pH changes and detergents, e.g., sodium dodecyl sulfate (SDS).[11,21,30,32] Special attention was devoted to the inhibition of these enzymes in order to suppress the browning of plants and fruits during storage.[12,33] Several inhibitors were found, one group acting as chelating agents for copper, e.g., CN^- or diethyldithiocarbamate, and the other acting as substrate analogues, e.g., phenyl thiourea or mimosine. In the food industry, the agent commonly used to inhibit enzymatic browning of grapes and other fruits is sulfite. However, the inhibition mechanism for sulfite is unclear. It may reduce the quinones back to the diphenols, inhibit CO directly, or react with quinones to form thioethers.[12] As CO is suggested to be involved in the plant defense system against wounding and diseases (see below), there is no guarantee that inhibition of this enzyme really leads to a better storage stability.

4. Crystal Structure of Sweet Potato CO[19]

Overall Structure and Folding. The structure of ibCO was solved and refined at 2.5 Å resolution in the *met* state (Cu(II)−Cu(II)). The enzyme has an ellipsoidal shape with axes of about 55, 45, and 45 Å. The secondary structure is dominated by α-helical regions (Figure 6). The most striking structural motif is a four-helix bundle surrounding the dinuclear copper site. In addition to these four helices, there are two helices closer to the surface. There are only small segments of β strand, most of them being located in the N-terminal region of the protein. This N-terminal region is linked to the rest of the enzyme by two disulfide bonds (Cys11−Cys28 and Cys27−Cys89). Besides these secondary structure features, the crystal structure reveals a high proportion of coiled regions.[19]

Coordination of the Dinuclear Copper Center. Both copper atoms forming the metal center are coordinated by three histidine N_ϵ atoms, as proposed on the basis of EXAFS measurements.[18] An unusual covalent thioether bond joins Cys92 to the Cu-coordinating His109 (Figure 4). An analogous thioether bridge has been reported to occur in TYR from *Neurospora crassa*, HC from *Helix pomatia*,[34,35] and in the crystal structure of HC from *Octopus dofleini*.[9] The Cys-His thioether bridge has been found only in type-3 copper proteins but does not seem to be essential, as it is absent from arthropodan HC crystal structures. A thioether bond between cysteine and tyrosine (Cys-Tyr) occurs in galactose oxidase, a type-2 copper protein, where it is thought to be involved in a radical reaction mechanism.[4,36] The involvement of the Cys-His bridge of CO in the catalytic pathway is possible, but a structural function is also under discussion.

The Different States of the Metal Center. The crystal structure of ibCO was solved in the two oxidation states relevant to the mechanism. Further, the structure of one inhibitor complex was solved to elucidate substrate binding.

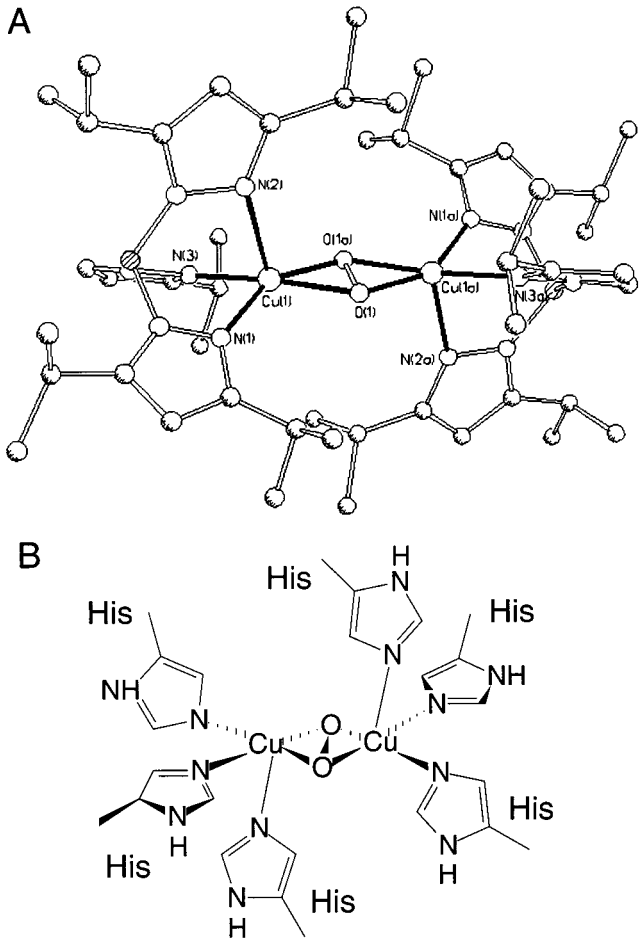

FIGURE 3. Dioxygen-binding mode as found (A) in a model compound[27] and (B) in the HC crystal structure from *Limulus polyphemus*.[8]

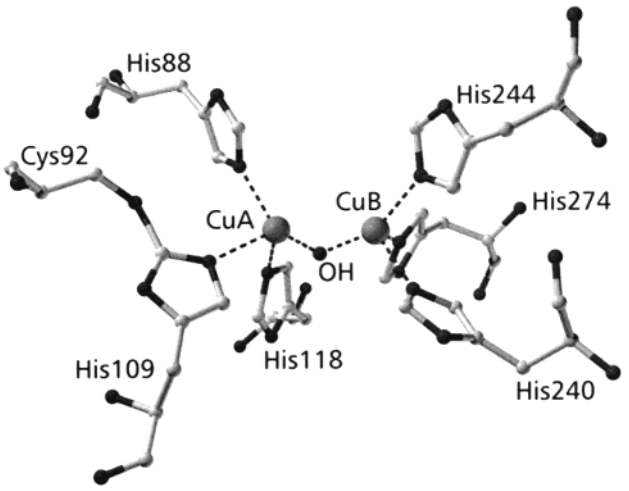

FIGURE 4. Coordination sphere of the dinuclear copper center in the met state.

***met* State.** In the *met* state (Cu(II), Cu(II)) the two cupric ions are at a distance of 2.9 Å, each of them being coordinated by three histidine residues. They are bridged by another atom—most likely a hydroxide ion—at a distance of about 1.8 Å from each cupric ion, so that each of them has a coordination number of 4 (Figure 4). This finding is supported by EXAFS measurements for the *met* form of ibCO and CO from gypsy wort.[14,18] The coordination sphere of each copper atom can be described as as trigonal pyramidal with His109 and His240 in the apical position, respectively.

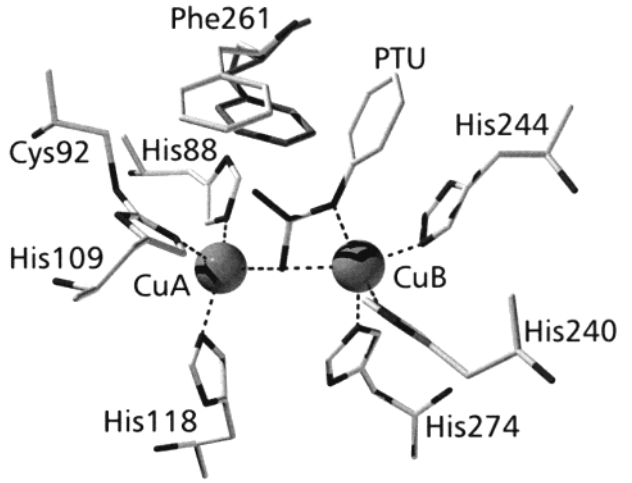

FIGURE 5. Crystal structure of the inhibitor complex of CO with PTU. Phe261 is shown additionally in the orientation of native CO (in dark color) to show rotation of Phe261 in the inhibitor complex (in light color).

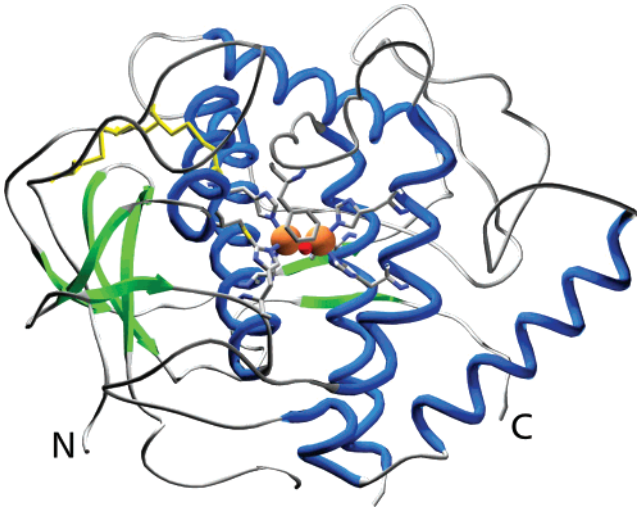

FIGURE 6. Overall structure of ibCO. Copper atoms are shown in orange, α helices in blue, β sheets in green, and disulfide bonds in yellow.

***deoxy* State.** In the *deoxy* or reduced state, both copper atoms are in the +I oxidation state. The copper−copper distance is 4.4 Å. The coordination numbers are 4 for CuA (three histidine ligands and a coordinating water molecule) and 3 for CuB (three histidine ligands). The coordination sphere is distorted trigonal pyramidal for CuA and square planar for CuB (the coordination site occupied by the bridging OH^- in the *met* state is vacant).

Inhibitor Complex. In the inhibitor complex with phenylthiourea (PTU), the copper−copper distance increases to 4.2 Å with the sulfur atom of PTU replacing the hydroxo bridge of the *met* state. The coordination spheres of the two coppers remain similar to those of the *met* state, but there are conformational changes at the

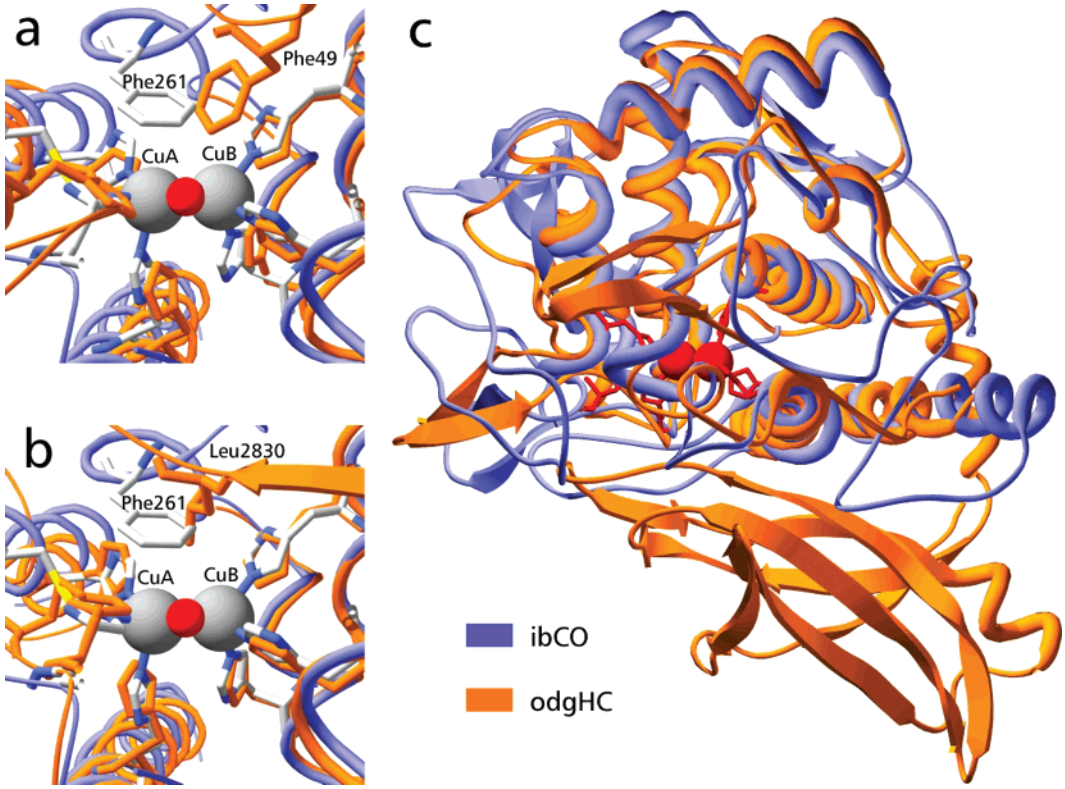

FIGURE 7. Comparison of 3D structures of CO and HC. Comparison of the active site of ibCO with those of HC from **(**a**)** *Limulus polyphemus* and **(**b**)** *Octopus dofleini*. Important residues (see text) and the copper atoms are labeled. **(c)** Comparison of the entire tertiary structures of ibCO and HC from *Octopus dofleini*. ibCO structure is shown in blue color and HC structures in orange color in all three figures.

active-site residues. The most significant change is a rotation of the aromatic ring of Phe261 (Figure 5).

Conclusions from the Structural Data. Compared with the *met* state, the coordinating residues have only slightly different positions in the reduced state, indicating a rather rigid pocket. The changes in coordination are associated with movements of the copper atoms in the pocket. The inhibitor complex shows that Phe261 is located above the active site like a gate, which rotates after the inhibitor is bound (Figure 5). Thus, access of the substrate to the catalytic metal center seems to be controlled by this "gate residue".

As a crystal structure of the *oxy* state of ibCO is not available so far, a model for substrate binding to *oxy*ibCO has been derived from the 3D structural data for *oxy*HC and the ibCO*PTU complex.[19] In this model, a monodentate binding mode of *o*-diphenol to CuB is preferred, consistent with Phe261 preventing the substrate from bridging the two copper atoms. On the other hand, an earlier model for TYR postulated bidentate binding of *o*-diphenol to both copper atoms.[5]

5. Structural Comparison of CO and HC

There are two classes of HC—arthropodan and molluscan—that differ in tertiary structure and subunit organization. Therefore, the ibCO crystal structure is compared with the two types of HC separately (Figure 7).

Arthropodan HC. Comparison of the ibCO structure with the two arthropodan HC structures (*Panulirus interruptus* and *Limulus polyphemus*) reveals that the HCs have an additional N-terminal domain. The size and position of this domain suggest that it acts as a shield, hindering the free access of phenolic substrates to the dicopper center. In both HC structures, a phenylalanine residue of the "shield region" reaches into the pocket of the oxygen-binding site (Figure 7a). In the case of *Limulus polyphemus* HC, Phe49 was shown to superimpose exactly on the position of the substrate in an ibCO−substrate complex, as modeled on the basis of a complex with the inhibitor PTU. Thus, there is strong evidence that Phe49 can block substrate binding.[19]

Molluscan HC. Much higher similarities of sequence and 3D structure are found when ibCO is compared with the only molluscan HC for which a structure is available, namely subunit *g* of the HC of the giant octopus *Octopus dofleini* (odgHC). The sequence identity between ibCO and odgHC is about 25%. However, the structural similarity is high,[34] despite the evolutionary distance between molluscs and higher plants: the tertiary structures are nearly identical overall, and the similarity is not limited to the four-helix bundle motif (Figure 7c). Again, the HC has a higher mass and shows an additional domain. The latter is in the C-terminal region, in contrast to the additional N-terminal domain of arthropodan HCs. As plants exhibit a C-terminal extension peptide (see above), it is suggested that this peptide inactivates precursor CO in a manner similar to the C-terminal "shield region" of odgHC. The structural similarity between the active sites of ibCO and odgHC is even closer than that between the

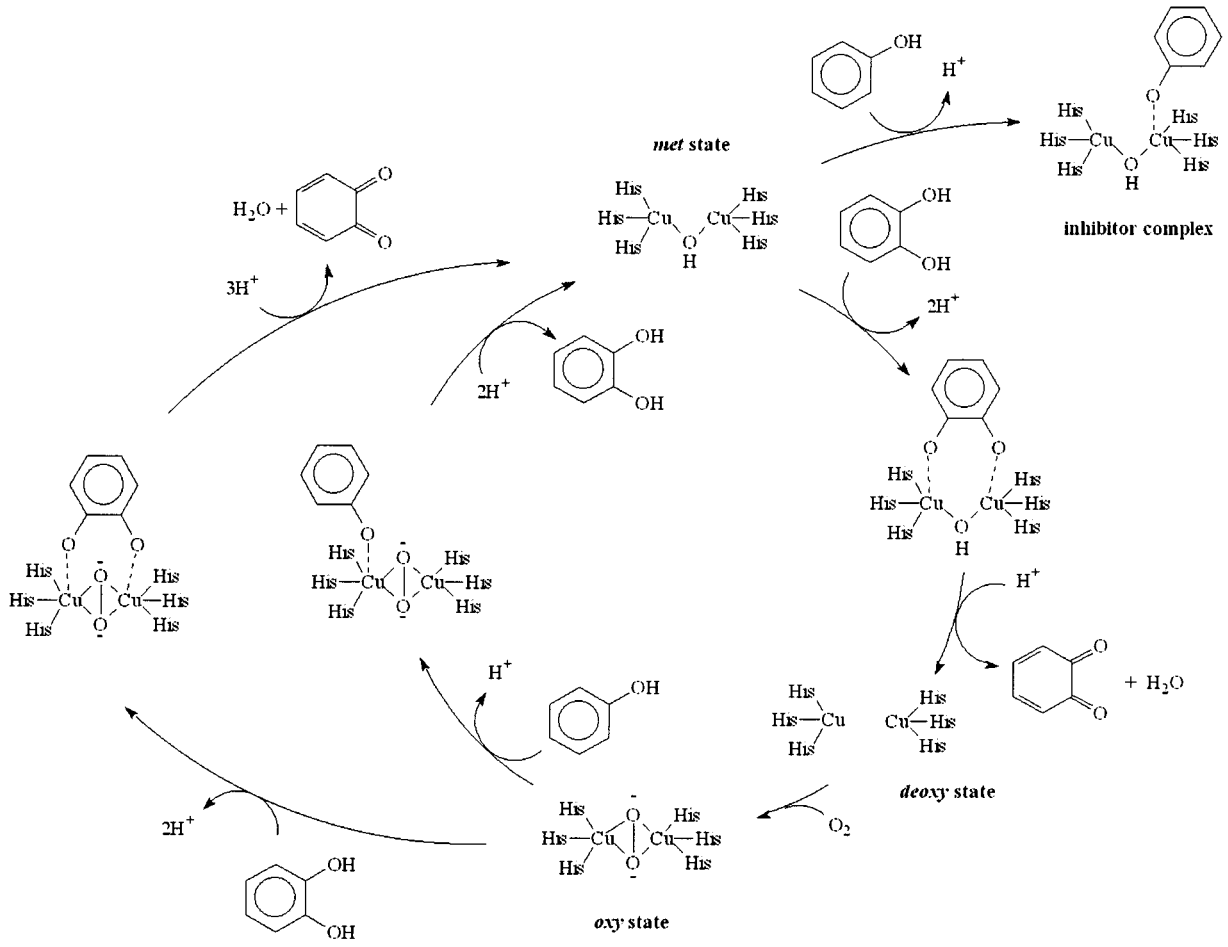

FIGURE 8. Mechanism of cresolase and catecholase activity of TYR and/or CO developed on the basis of an initial proposal by Solomon and co-workers[5] and including more recent results.[30,34]

active sites of ibCO and *Limulus polyphemus* HC. The odgHC structure has the same Cys-His link as ibCO, resulting in an identical coordination of CuA (Figure 7b). The substrate-blocking residue Phe49 in *Limulus polyphemus* HC corresponds to Leu2830 in odgHC. This leucine residue may block diphenols less effectively than phenylalanine and may thus be responsible for a weak catecholase activity detected in HC from another octopus subspecies (*Octopus vulgaris*).[22] Since the structural similarity of the two *Octopus* HCs is not known yet, this conclusion remains speculative.

6. Proposed Reaction Pathway

The catalytic mechanism of TYR was first studied in detail by Solomon and co-workers.[5] Solomon proposed a mechanism for both the cresolase and catecholase activities of TYR (Figure 8). This mechanism suggests the *oxy* state to be the starting point of cresolase activity (inner circle). This state is present in the resting form of TYR in a proportion of about 15% (85% *met* state). A monophenol substrate binds to the *oxy* state and is monooxygenated to *o*-diphenol. This diphenol subsequently binds to the copper center of *met*TYR in a bidentate binding mode proposed on the basis of a model compound.[26] Oxidation of the diphenol substrate leads to the reduced state of the dinuclear copper center. Reoxidation of the reduced state to the *oxy* state occurs by attack of dioxygen and closes the catalytic cycle.

The mechanism of catecholase activity (outer circle) starts from the *oxy* and *met* states. A diphenol substrate binds to the *met* state (for example), followed by the oxidation of the substrate to the first quinone and the formation of the reduced state of the enzyme. Binding of dioxygen leads to the *oxy* state, which is subsequently attacked by the second diphenol molecule. Oxidation to the second quinone forms the *met* state again and closes the catalytic cycle.

Alternative reaction mechanisms[30] include a radical mechanism proposed by Kitajima and Moro-oka[27] and a mechanism involving a Cu(III) intermediate based on measurements of model compounds.[37] On the basis of the crystal structure of the ibCO−PTU inhibitor complex, monodentate binding of the substrate was suggested for CO.[19] A radical mechanism, as proposed for the weak catecholase activity found in *Octopus vulgaris* HC,[22] is also possible for CO, due to the strong structural relationship between ibCO and odgHC as described above.

The distinct difference between CO and TYR has not yet been explained. A lag phase in the monophenolase activity of TYR has been found and studied and is

proposed to be a result of temporary inhibition of the *met* state of TYR by excess of the monophenol substrate (Figure 8).[30] Monophenolase activity increases when the diphenol product displaces the monophenol from *met*TYR and allows the continuation of the catalytic cycle. CO in its isolated form is present exclusively in the *met* state and is also inhibited by phenol.[18] It was therefore suggested that lack of the *oxy* state is the reason CO lacks cresolase activity. As *oxy*CO also shows no monooxygenase activity (B. Krebs, unpublished data), this explanation does not seem entirely satisfying. Another possible reason is that access to CuA, which has been proposed to be necessary for the oxygenation of monophenols,[21] is blocked in the ibCO crystal structure.

7. Physiological Role

Several functions for COs in higher plants have been proposed. There is increasing evidence, but not yet a proof, for some of them. As several isozymes are sometimes found in a single organism, COs may have different functions depending on their location.[12]

Photosynthesis. Plant COs have often been found tightly bound to the thylakoid membranes,[11,12] and nearly all COs contain a transit peptide targeting to the internal lumen of the thylakoid membrane in plastids.[20] Transport into the chloroplasts and proteolytic cleavage of this transit peptide were performed in vivo and in vitro for CO from tomato, maize, and pea. The transport leads to the thylakoid lumen in a two-cleavage-step mechanism typical for thylakoid lumen proteins.[38] CO has been found to be nuclear encoded but still inactive until incorporated into the plastids, indicating a role in photosynthesis.[12]

Flower Coloration. Recently there has been a report on an auresidin synthase which is involved in the synthesis of aurones, i.e., flavonoids that provide yellow color to the flowers of some plants.[39] This CO homologue (or PPO homologue as stated in the original citation) has a sequence identity of about 45% with other plant COs. In contrast to CO, auresidin synthase is a glycoprotein and does not have a plastid transit peptide. It is therefore supposed to be localized in the vacuole.

Plant Disease Resistance. The most plausible function proposed for plant COs is a role in the disease resistance of higher plants. The enzyme is cytosolic or membrane-bound, whereas possible substrates are kept separated in the vacuole. After disruption of the cell by wounding or infection, the membrane is lysed, and these two components can come in contact. This causes the formation of quinones which spontaneously polymerize to melanins. CO mRNA has been found to be upregulated after wounding or infecting, e.g., in apples. Further, some parasites have been found to use inhibitors of the CO, indicating that the CO/diphenol system is an obstacle against the colonisation of the host.[12]

Functions of TYRs. In contrast to the confusion surrounding the function of plant COs, there is no controversy concerning the function of TYRs in mammals and insects. In mammals, TYR initiates the formation of pigmentation. The absence or inactivation of the enzyme leads to forms of albinism (tyrosinase-negative albinism and occultaneous albinism). In insects, TYRs are involved in sclerotisation, i.e., the hardening of the chitinous cuticle, and defense.[12]

We thank the Deutsche Forschungsgemeinschaft for financial support. Thanks are due to Annette Rompel for helpful discussions and to Beate Jasper for much practical help. Thanks also to Prof. Hans Freeman for valuable suggestions.

References

(1) Malmström, B. G. Enzymology of oxygen. *Annu. Rev. Biochem.* **1982**, *51*, 21−59.
(2) Shepard, W. E. B.; Anderson, B. F.; Lewandoski, G. E.; Norris, D. N.; Baker, J. Copper coordination geometry in azurin undergoes minimal change on reduction of copper(II) to copper(I). *J. Am. Chem. Soc.* **1990**, *112*, 7817−7819.
(3) Lippard, S. J.; Berg, J. M. *Principles of Bioinorganic Chemistry*; University Science Books: Mill Valley, CA, 1994.
(4) Adman, E. T. Copper protein structures. *Adv. Protein Chem.* **1991**, *42*, 145−197.
(5) Solomon, E. I.; Sundaram, U. M.; Machonkin, T. E. Multicopper oxidases and oxygenases. *Chem. Rev.* **1996**, *96*, 2563−2605.
(6) van Holde, K. E.; Miller, K. I. Hemocyanins. *Adv. Protein Chem.* **1995**, *47*, 1−81.
(7) Gaykema, W. P. J.; Hol, W. G. J.; Vereijken, J. M.; Soeter, N. M.; Bak, H. J.; Beintema, J. J. 3.2 Å structure of the copper-containing, oxygen-carrying protein *Panulirus interruptus* hemocyanin. *Nature* **1984**, *309*, 23−29.
(8) Magnus, K. A.; Ton-That, H.; Carpenter, J. E. Recent structural work on the oxygen-transport protein hemocyanin. *Chem. Rev.* **1994**, *94*, 727−735.
(9) Cuff, M. E.; Miller, K. I.; van Holde, K. E.; Hendrickson, W. A. Crystal structure of a functional unit from *Octopus* hemocyanin. *J. Mol. Biol.* **1998**, *278*, 855−870.
(10) Hughes, A. L. Evolution of the arthropod prophenoloxidase/hexamerin protein family. *Immunogenetics* **1999**, *49*, 106−114.
(11) Mayer, A. M.; Harel, E. Polyphenol oxidases in plants. *Phytochemistry* **1979**, *18*, 193-215.
(12) Walker, J. R.; Ferrar, P. H. Diphenol oxidases, enzyme-catalysed browning and plant disease resistance. *Biotechnol. Genet. Eng. Rev.* **1998**, *15*, 457−498.
(13) Mayer, A. M. Polyphenol oxidases in plants−recent progress. *Phytochemistry* **1987**, *26*, 11−20.
(14) Rompel, A.; Fischer, H.; Meiwes, D.; Büldt-Karentzopoulos, K.; Dillinger, R.; Tuczek, F.; Witzel, H.; Krebs, B. Purification and spectroscopic studies on catechol oxidases from *Lycopus europaeus* and *Populus nigra*: evidence for a dinuclear copper center of type 3 and spectroscopic similarities to tyrosinase and hemocyanin. *J. Biol. Inorg. Chem.* **1999**, *4*, 56−63.
(15) Jiang, Y. M.; Fu, J. R.; Zauberman, G.; Fuchs, Y. Purification of polyphenol oxidase and the browning control of litchi fruit by glutathione and citric acid. *J. Sci. Food Agric.* **1999**, *79*, 950−954.
(16) Hyodo, H.; Uritani, I. Properties of polyphenol oxidases produced in sweet potato tissue after wounding. *Arch. Biochem. Biophys.* **1967**, *122*, 299−309.
(17) Wang, Z. X.; Li, S. M.; Loscher, R.; Heide, L. 4-Coumaroyl coenzyme A 3-hydroxylase activity from cell cultures of *Lithospermum erythrorhizon* and its relationship to polyphenol oxidase. *Arch. Biochem. Biophys.* **1997**, *347*, 249−255.
(18) Eicken, C.; Zippel, F.; Büldt-Karentzopoulos, K.; Krebs, B. Biochemical and spectroscopic characterization of catechol oxidase from sweet potatoes (*Ipomoea batatas*) containing a type-3 dicopper center. *FEBS Lett.* **1998**, *436*, 293−299.
(19) Klabunde, T.; Eicken, C.; Sacchettini, J. C.; Krebs, B. Crystal structure of a plant catechol oxidase containing a dicopper center. *Nat. Struct. Biol.* **1998**, *5*, 1084−1090.
(20) van Gelder, C. W. G.; Flurkey, W. H.; Wichers, H. J. Sequence and structural features of plant and fungal tyrosinases. *Phytochemistry* **1997**, *45*, 1309−1323.
(21) Decker, H.; Tuczek, F. Tyrosinase/catecholoxidase activity of hemocyanins: structural basis and molecular mechanism. *Trends Biochem. Sci.* **2000**, *25*, 392−397.
(22) Salvato, B.; Santamaria, M.; Beltramini, M.; Alzuet, G.; Casella, L. The enzymatic properties of *Octopus vulgaris* hemocyanin: o-diphenol oxidase activity. *Biochemistry* **1998**, *37*, 14065−14077.

(23) Espín, J. C.; Tudela, J.; García-Canovas, F. 4-Hydroxyanisole: the most suitable monophenolic substrate for determining spectrophotometrically the monophenolase activity of polyphenol oxidase from fruits and vegetables. *Anal. Biochem.* **1998**, *259*, 118−126.
(24) Gerdemann, C.; Eicken, C.; Magrini, A.; Meyer, H. E.; Rompel, A.; Spener, F.; Krebs, B. Isozymes of *Ipomoea batatas* catechol oxidase differ in catalase-like activity. *Biochim. Biophys. Acta* **2001**, *1548*, 94−105.
(25) Bubacco, L.; Salgado, J.; Tepper, A. W.; Vijgenboom, E.; Canters, G. W. ^{1}H NMR spectroscopy of the binuclear Cu(II) active site of *Streptomyces antibioticus* tyrosinase. *FEBS Lett.* **1999**, *442*, 215−220.
(26) Karlin, K. D.; Kaderli, S.; Zuberbühler, A. D. Kinetics and thermodynamics of copper(I)/dioxygen interaction. *Acc. Chem. Res.* **1997**, *1997*, 139−147.
(27) Kitajima, N.; Moro-oka, Y. Copper-dioxygen complexes—Inorganic and bioinorganic perspectives. *Chem. Rev.* **1994**, *94*, 737−757.
(28) Kodera, M.; Katayama, K.; Tachi, Y.; Kano, K.; Hirota, S.; Fujinami, S.; Suzuki, M. Crystal structure and reversible O_2-binding of a room-temperature stable μ-$\eta^2\eta^2$-peroxodicopper(II) complex of a sterically hindered hexapyridine dinucleating ligand. *J. Am. Chem. Soc.* **1999**, *121*, 11006−11007.
(29) Monzani, E.; Battaini, G.; Perotti, A.; Casella, L.; Gullotti, M.; Santagostini, L.; Nardin, G.; Randaccio, L.; Geremia, S.; Zanello, P.; Opromolla, G. Mechanistic, structural, and spectroscopic studies on the catecholase activity of a dinuclear copper complex by dioxygen. *Inorg. Chem.* **1999**, *38*, 5359−5369.
(30) Sánchez-Ferrer, A.; Rodriguez-Lopez, J. N.; García-Cánovas, F.; García-Carmona, F. Tyrosinase: a comprehensive review of its mechanism. *Biochim. Biophys. Acta* **1995**, *1247*, 1−11.
(31) Rompel, A.; Fischer, H.; Meiwes, D.; Büldt-Karentzopoulos, K.; Magrini, A.; Eicken, C.; Gerdemann, C.; Krebs, B. Substrate specificity of catechol oxidase from *Lycopus europaeus* and characterization of the bioproducts of enzymic caffeic acid oxidation. *FEBS Lett.* **1999**, *445*, 103−110.
(32) Jiménez, M.; García-Carmona, F. Kinetics of the slow pH-mediated transition of polyphenol oxidase. *Arch. Biochem. Biophys.* **1996**, *331*, 15−22.
(33) Artes, F.; Castaner, M.; Gil, M. I. Review: Enzymatic browning in minimally processed fruit and vegetables. *Food Sci. Technol. Int.* **1998**, *4*, 377−389.
(34) Eicken, C.; Krebs, B.; Sacchettini, J. C. Catechol oxidase—structure and activity. *Curr. Opin. Struct. Biol.* **1999**, *9*, 677−683.
(35) Halcrow, M. A. Chemically modified amino acids in copper proteins that bind or activate dioxygen. *Angew. Chem., Int. Ed.* **2001**, *40*, 346−349.
(36) Stubbe, J.; van der Donk, W. A. Protein radicals in enzyme catalysis. *Chem. Rev.* **1998**, *98*, 705−762.
(37) Holland, P. L.; Tolman, W. B. Dioxygen activation by copper sites: relative stability and reactivity of (μ-η^2:η^2-peroxo)- and bis-(μ-oxo)dicopper cores. *Coord. Chem. Rev.* **1999**, *192*, 855−869.
(38) Sommer, A.; Ne'eman, E.; Steffens, J. C.; Mayer, A. M.; Harel, E. Import, targeting, and processing of a plant polyphenol oxidase. *Plant Physiol.* **1994**, *105*, 1301−1311.
(39) Nakayama, T.; Yonekura-Sakakibara, K.; Sato, T.; Kikuchi, S.; Fukui, Y.; Fukuchi-Mizutani, M.; Ueda, T.; Nakao, M.; Tanaka, Y.; Kusumi, T.; Nishino, T. Aureusidin synthase: A polyphenol oxidase homolog responsible for flower coloration. *Science* **2000**, *290*, 1163−1166.

AR990019A